Molecular Adjustment of the Electronic Properties of Nanoporous Electrodes in Dye-Sensitized Solar Cells

Sven Rühle,[†] Miri Greenshtein,[‡] S.-G. Chen,[‡] Alexandra Merson,[§] Hillel Pizem,[‡] Chaim S. Sukenik,[‡] David Cahen,*[,†] and Arie Zaban*[,‡]

Department of Materials and Interfaces, Weizmann Institute of Science, Rehovot 76100, Israel, Department of Chemistry, Bar-Ilan University, Ramat-Gan 52900, Israel, and School of Electrical Engineering, Tel Aviv University, Ramat-Aviv 69978, Israel

Received: March 17, 2005; In Final Form: June 22, 2005

Molecular modification of dye-sensitized, mesoporous TiO_2 electrodes changes their electronic properties. We show that the open-circuit voltage (V_{oc}) of dye-sensitized solar cells varies linearly with the dipole moment of coadsorbed phosphonic, benzoic, and dicarboxylic acid derivatives. A similar dependence is observed for the short-circuit current density (I_{sc}). Photovoltage spectroscopy measurements show a shift of the signal onset as a function of dipole moment. We explain the dipole dependence of the V_{oc} in terms of a TiO_2 conduction band shift with respect to the redox potential of the electrolyte, which is partially followed by the energy level of the dye. The I_{sc} shift is explained by a dipole-dependent driving force for the electron current and a dipole-dependent recombination current.

Introduction

Dye-sensitized, nanocrystalline, solar cells (DSSC) based on mesoporous TiO_2 films are a potential low-cost alternative to single or polycrystalline $p-n$ junction solar cells and can reach light to electric power conversion efficiencies of about 11%.[1] During cell operation dye molecules inject electrons from their excited state into the conduction band (CB) of the TiO_2 particles.[2] The energy difference between the excited dye state and the CB of the TiO_2,[3] the bonding between dye and semiconductor[4−6] and the properties of the redox couple in the electrolyte[4] affect the efficiency of the cell. One of the most fundamental properties for the design of DSSCs is the energy level alignment at the semiconductor/dye/electrolyte interface. Previously, it was shown[7] that the redox potential of adsorbed dye depends on the pH of the electrolyte and on the potential applied to the semiconductor. The energy level of the dye with respect to the TiO_2 CB depends on the ionic double layer that is formed at the TiO_2/electrolyte interface. If the dye is located inside the ionic double layer, its redox potential tends to follow the changes of the semiconductor potential. However, if the dye is mainly outside the double layer, its potential will be almost independent of the semiconductor potential.

Control of the semiconductor CB level (E_{CB}) will affect the efficiency of the DSSC. A shift of E_{CB} toward the vacuum level (i.e., away from the redox potential of the electrolyte, E_{redox}) results in a higher open-circuit voltage (V_{oc}),[8,9] which can improve the efficiency of the cell. To keep the DSSC operational, E_{CB} has to remain below some excited dye states to enable electron injection into the semiconductors CB.[10] The ability to shift E_{CB} toward E_{redox} will decrease the V_{oc} but might be desirable for more attractive dyes (lower production cost, better stability, higher absorption coefficient) that cannot inject well into TiO_2 since their excited-state potential is not sufficiently above E_{CB} of TiO_2. In this case, lowering E_{CB} (bringing it closer to E_{redox}) will enable electron injection from a wider variety of dyes to the semiconductor as long as the dye energy levels do not fully follow the shift of E_{CB}.

Organic molecules with different dipole moments, adsorbed to the surface of semiconductors, can modify the electronic properties such as band bending, electron affinity (χ) and work function (Φ) of the semiconductor.[11] This has been used to modify the $I-V$ characteristics of ZnO/Au Schottky junctions,[12] CdS/CdTe solar cells[13,14] and other solid-state systems.[15−17] It was furthermore reported that also the relative energetics at an organic/inorganic heterojunction, comprised of a compact TiO_2 layer (n-type) and an organic p-type semiconductor compound (spiro-OMeTAD), could be modified by an organic dipole layer.[18]

To the best of our knowledge, this kind of surface modification has not yet been applied to electrochemical systems such as DSSCs with nanoporous TiO_2/liquid electrolyte interface. Here we report on a way to control the TiO_2 energy levels by adsorption of a series of organic molecules with different dipole moments, together with the dye molecules. The V_{oc}, the short-circuit photocurrent, I_{sc}, and the dark conductivity of cells made with molecular modified electrodes, as well as photovoltage spectroscopy measurements of those electrodes, show a clear correlation with the molecular dipole moment. These results can be explained consistently in terms of a dipole-related shift of E_{CB} with respect to E_{redox}.

Materials and Methods

Preparation of TiO_2 Electrodes. TiO_2 slurries, consisting of 23 nm sized particles (characterized by X-ray diffraction (XRD) and transmission electron microscopy (TEM)), were synthesized by a standard hydrothermal method.[19] In brief, titanium tetraisopropoxide, dissolved in 2-propanol, was hy-

* Corresponding authors: Telephone: (D.C.) +972-8-934-2246; (A.Z.) +972-3-5317876. E-mail: (D.C.) david.cahen@weizmann.ac.il; (A.Z.) zabana@mail.biu.ac.il.

[†] Weizmann Institute of Science.

[‡] Bar-Ilan University.

[§] Tel Aviv University.

10.1021/jp0514123 CCC: $30.25
Published on Web 09/17/2005

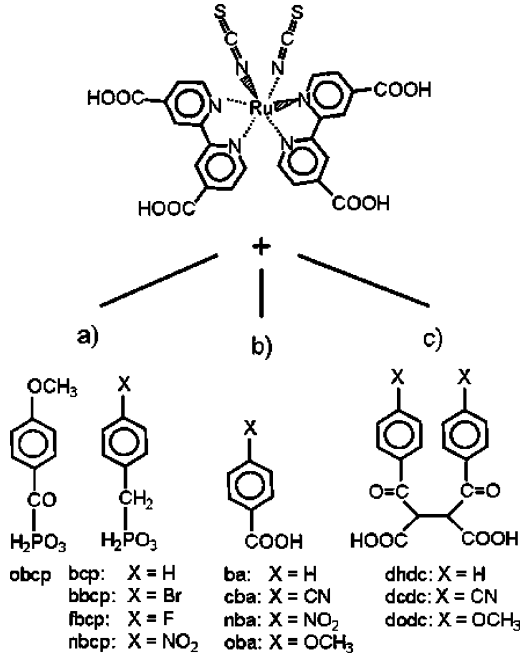

Figure 1. Molecules used for molecular modification of dye-sensitized TiO_2 electrodes: (a) phosphonic acid derivatives with different functional groups indicated with X; (b) benzoic acid derivatives; (c) dicarboxylic acid derivatives.

drolyzed in acetic acid at pH 2. After overnight stirring, the 2-propanol was evaporated at 82 °C and the suspension was autoclaved at 250 °C for 13 h.

Glass substrates covered with conducting F-doped SnO_2 (FTO, Libby Owens Ford, 8 Ω/square) were cleaned with soap, rinsed with deionized water (18.2 MΩ), and dried in an air stream.[19] The TiO_2 suspension was spread on the conducting glass substrates by a glass rod, using adhesive tape as spacers. After drying the films in air, they were sintered in air at 450 °C for 30 min. The TiO_2 films thickness was 3 μm, as measured with a Surftest SV 500 profilometer (Mitutiyi Co). The crystal structure of the nanoparticles (anatase) was determined with a Bruker D8 X-ray diffractometer.

Dye Adsorption and Molecular Modification of TiO_2 Electrodes. Mesoporous dye-sensitized TiO_2 electrodes where molecularly modified with a two- or one-step coadsorption method (methods A and B, respectively), depending on the size of coadsorbed molecules. For conductivity measurements mesoporous TiO_2 electrodes (without dye) were electrochemically modified (method C).

Method A. Phosphonic acid derivatives (see Figure 1a) were coadsorbed onto TiO_2 electrodes that were already sensitized with the dye (a two-step process). The dye [*cis*-bis(isothiocyanato)bis(4,4-dicarboxy-2,2-bipyridine)ruthenium(II)] (also known as N3) was purchased from Solaronix SA Co. For dye sensitization, mesoporous TiO_2 films were preheated to 150 °C, cooled to 80 °C, and immersed overnight in an ethanol solution containing 0.5 mM N3. In a second step, the dye-sensitized TiO_2 electrodes were modified by immersion into 5 mL 10^{-5} M ethanol solution containing one of the indicated phosphonic acid derivatives. Adsorption isotherms were measured to control the surface coverage of coadsorbed phosphonic acid. This involved monitoring the light absorption of the phosphonic acid in solution at 253−308 nm, depending on the specific acid (HP 8453 UV−vis spectrophotometer). The electrode was immersed in a cuvette, containing the solution in a way so that it did not interfere with the light beam (see insert of Figure 2). The decrease of the phosphonic acid concentration in the solution

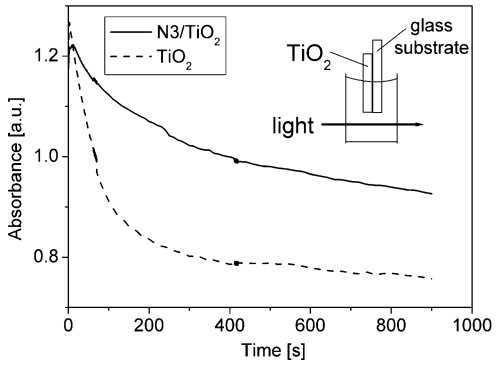

Figure 2. Typical adsorption rate measurement of phosphonic acids by way of change of optical absorption at 300 nm of nitrobenzenephosphonic acid in solution, during its adsorption onto bare and onto N3-sensitized TiO_2 films.

TABLE 1: Series of Organic Molecules, Used in This Work, with the Dipole Moments of the Free Molecules and the Abbreviations Used for the Molecules

name	abbreviation	free molecule dipole moment (D)
phosphonic acid derivatives		
benzenephosphonic acid	bcp	−1.36
methoxybenzenephosphonic acid	obcp	−1.16
bromobenzenephosphonic acid	bbcp	+1.97
fluorobenzenephosphonic acid	fbcp	+2.91
nitrobenzenephosphonic acid	nbcp	+5.10
benzoic acid derivatives		
benzoic acid	ba	−2.04
cyanobenzoic acid	cba	+3.70
nitrobenzoic acid	nba	+3.53
methoxybenzoic acid	oba	−3.70
dicarboxylic acid derivatives		
dicarboxylic acid	dhdc	−3.45
dicyanodicarboxylic acid	dcdc	+2.72
dimethoxydicarboxylic acid	dodc	−4.92

constitutes a measure of phosponic acid adsorption on the porous TiO_2 electrode.

Benzoic acid derivatives (see Figure 1b) were coadsorbed in a similar two-step process. Dye-sensitized electrodes were immersed for 12 h into solutions that contained 0.5 mM of the benzoic acid derivates dissolved in acetonitrile (ACN). Desorption of dye molecules into the ACN was found to be negligible such that monitoring of the adsorption and dye-desorption process such as that above was not needed.

Method B. Dicarboxylic acid derivatives (see Figure 1c) were adsorbed in a one-step process from an ethanol solution that contained the dye (0.5 mM) together with the respective dicarboxylic acid derivative (0.3 mM). To minimize surface-adsorbed water, the films were heated to 150 °C and cooled to 80 °C as in method A, before they were immersed in the ethanol solution (overnight). After adsorption the films were rinsed with ethanol and dried in a nitrogen stream.

The derivatives used in this work, their abbreviations, and dipole moments are summarized in Table 1, and the molecules are schematically depicted in Figure 1. The different functional groups of these molecules each contribute to the molecular dipole moments. The values of these dipole moments were calculated as described elsewhere.[16]

Method C. TiO_2 films were molecularly modified by electrochemical deposition of benzenediazonium tetrafluoroborate derivatives, as described elsewhere.[20] These molecules carried the same functional groups as some of the phosphonic, benzoic, or dicarboxylic acids, used in methods A and B.

V_{oc}, I_{sc}, and IPVE Measurements. A sandwich-type configuration was used to measure the performance of molecular

modified DSSCs, using Pt-coated, conducting FTO glass as counter electrode, which was separated from the TiO_2 electrode by Teflon tape. The electrolyte consisted of 0.5 M LiI/0.05 M I_2 dissolved in a mixture of ACN and 3-methyl-2-oxazolidinone in a 1:1 mixing ratio. The active cell area of about 1 cm^2 was illuminated with a xenon or halogen lamp. Typical cell performance without molecular modification (under simulated AM 1.5 illumination) was $I_{SC} \sim 12$ mA/cm^2, $V_{OC} \sim 670$ mV, FF 65−70%, yielding an approximate efficiency of 5%.

The TiO_2 PVS spectra were measured by a luminescence spectrometer. The V_{oc} measurements were performed with a potentiostat (Eco Chemie, model PGSTAT20). Optical transmission and absorption spectra of the molecular modified, dye-sensitized TiO_2 electrodes were measured with a spectrophotometer (Jasco V-570 or Cary 500).

Dark Conductivity Measurements. Steady-state electron transport measurements were performed on the TiO_2 films that were modified by method C. The TiO_2 films were deposited onto interdigitated gold electrodes which were separated by an insulating gap of about 10 μm (so-called interdigitated microelectrodes). A schematic cross-section drawing is shown in Figure 10a. The resistivity of the molecular modified TiO_2 films was measured with a bipotentiostat system (Autolab), where the two gold electrodes were connected as working electrode one and two (WE_1 and WE_2).[21−23] A constant potential difference between WE_1 and WE_2 was applied (usually 50 mV), while an external potential was applied with respect to an Ag/AgCl reference electrode (RE). A Pt sheet was used as counter electrode (CE). An aqueous 0.5 M NaCl solution was used as an electrolyte, which is different from the electrolyte used for DSSC measurements (see above) to avoid redox electrochemistry, associated with the DSSC electrolyte, which would interfere with the measurements. A more detailed description of the measurement configuration and procedure can be found elsewhere.[23]

Results and Discussion

Molecular Modification. The absorption change of the phosphonic acid in solution was measured to monitor molecular modification with phosphonic acid derivatives. Figure 2 shows the absorbance at 300 nm, where the phosphonic acids have an absorption peak, when a bare (dashed line) and a dye-sensitized (solid line) electrode were immersed into the solution. The slower decrease of the solid line indicates that less adsorption sites are available on the dye-sensitized electrode than on the bare TiO_2. Voids between surface-adsorbed N3 molecules, due to steric hindrance as a result of the shape of the N3 molecule (cf. Figure 1), as well as a slight desorption of N3 molecules, create the available adsorption sites.

The number of phosphonic acid molecules, coadsorbed onto the TiO_2 electrode, was calculated from the change in the optical absorption as shown in Figure 2. By monitoring solution absorption at both 300 and 540 nm, we could confirm that similar concentrations of phosphonic acids were adsorbed onto each electrode, while at the same time ensuring that the dye density, left on the TiO_2 surfaces after phosphonic acid adsorption, did not vary significantly. The surface area of the TiO_2, which is required for the calculation of the surface density of dipoles, N, was estimated from (1) the optical absorption of the dye-modified electrode in comparison with a bare one, using the known absorption coefficients of a dye monolayer,[24] and (2) using the crystal size and film thickness, assuming spherical particles and an ordered system. In this way we estimate a surface density of dipole molecules of around 2×10^{13} cm^{-2}.

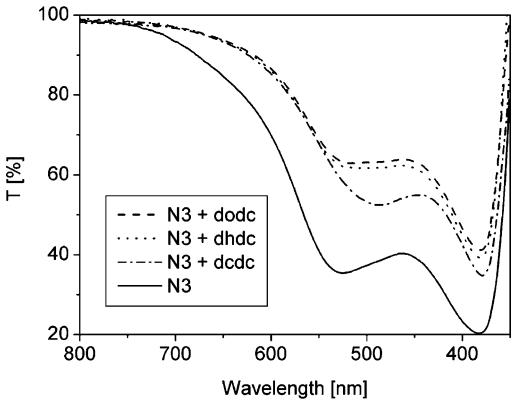

Figure 3. Optical absorption spectra of N3-covered electrodes, modified with dicarboxylic acid derivatives.

Electrodes, modified with phosphonic acid derivatives did not show any significant differences in the optical absorption spectrum of the N3 dye. The same was found for electrodes, modified with benzoic acid derivatives, because of negligible N3 desorption into the ACN solvent (not shown). From this we deduce that the concentration of surface-adsorbed dye molecules was not significantly changed by the two-step modification process and that these molecules adsorbed only to vacant binding sites between the dye molecules.

For dicarboxylic acid derivatives a one-step modification process was chosen. The dicarboxylic acid molecules are larger (two binding sites and thus a larger footprint), which would lead in a two-step process to a rather low adsorption between the dye molecules, due to geometrical restrictions. In the one-step adsorption process dicarboxylic acid derivatives compete with N3 molecules for binding sites. As a result the total amount of N3 molecules is now lower than after the two-step modification process. Indeed, electrodes, modified in the one-step method (B) show a lower light absorption than an unmodified N3 electrode, as can be seen from the transmission spectra in Figure 3. In contrast electrodes modified by the two-step method (A) have a dye coverage that is nearly identical to that of unmodified N3 electrodes (not shown).

I_{sc} and V_{oc} of Molecularly Modified DSSCs. Open-circuit voltages and short-circuit currents of molecularly modified DSSCs as a function of the molecular dipole moment are shown in Figure 4a−c. The I_{sc} values are normalized to the short-circuit current of the unmodified N3 reference (I_{sc}(N3)). Electrodes modified in a two-step process (Figure 4a,b) show a normalized I_{sc} around one, which is consistent with the very similar N3 coverage of modified and unmodified samples. In contrast samples modified in a one-step process show significantly smaller normalized I_{sc} values (0.25−0.55), due to the smaller concentration of dye adsorbed on the surface (see Figure 3). Within each series of molecules both V_{oc} and I_{sc} increase, if the dipole moment of the coadsorbed species points toward the TiO_2 surface. Molecules with a dipole moment pointing away from the surface lead to a decrease in I_{sc} and V_{oc}. We observe a V_{oc} shift of ∼8.6 mV/D for the phosphonic acid series, ∼7.3 mV/D for benzoic acids, and a shift of ∼6.7 mV/D for dicarboxylic acid derivatives. No systematic dipole-related effects were found on the fill factor.

We attribute these changes in V_{oc} to the dipole moment of the coadsorbed species and emphasize that a difference in N3 coverage cannot explain this effect. As mentioned above no difference of N3 coverage could be observed in the absorption spectra of phosphonic and benzoic acid modified samples (method A). In contrast dicarboxylic acid modified electrodes

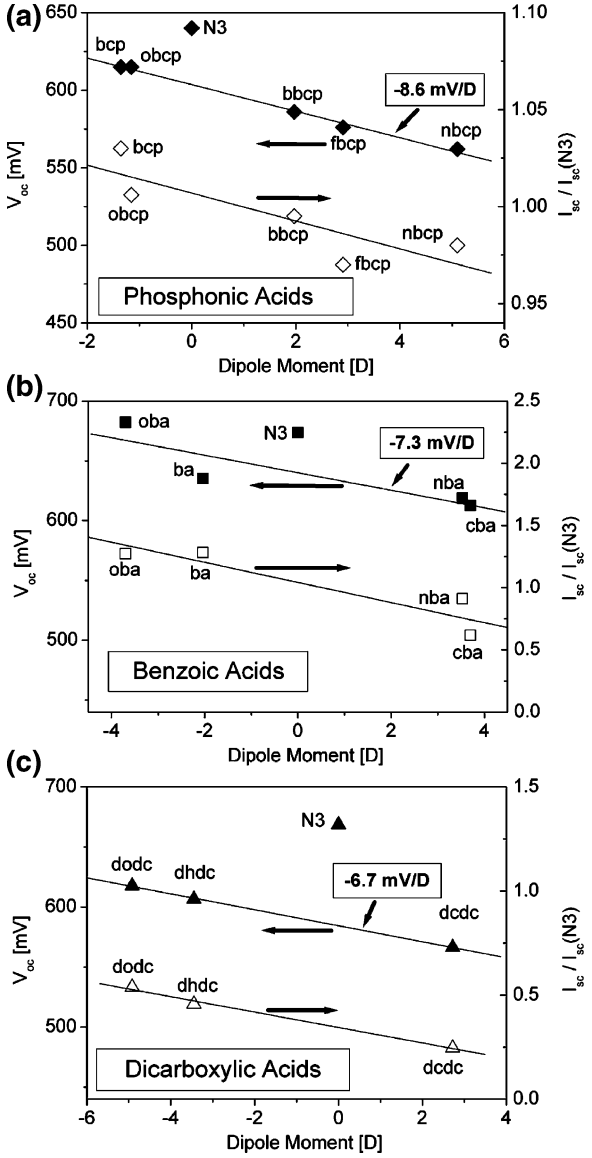

Figure 4. (a) Open-circuit voltage, V_{oc}, and short-circuit current, I_{sc}, measurements of dye-sensitized TiO_2 electrodes, modified in a two-step process with phosphonic acid derivatives. I_{sc} values are normalized to the short-circuit current of the unmodified electrode, I_{sc}(N3). (b) Same as panel a for dye-sensitized electrodes, modified in a two-step process with benzoic acid derivatives. (c) Same as panels a and b for dye-sensitized electrodes, modified in a one-step process with dicarboxylic acid derivatives.

(method B) show small variations in the N3 coverage as shown in Figure 3. However, by comparing the transmission curves with the V_{oc} and I_{sc} measurements, we can see that the slight differences in N3 concentration are overcompensated by the dipole effect. Thus, the dodc modified electrode shows a *higher* I_{sc} and V_{oc} while it has a *lower* dye coverage compared to the dhdc and dcdc modified electrodes!

The change in the V_{oc} can be explained qualitatively by a dipole-related shift of E_{CB} with respect to the redox potential of the electrolyte (E_{redox}). This effect is shown in terms of energy level/band level diagrams of the TiO_2 nanoparticle/electrolyte interface (Figure 5a−c). The V_{oc} in DSSCs is limited mainly by the energy difference between E_{CB} and E_{redox},[25,26,9] as shown in Figure 5a. In that figure the dipole of the molecular layer at the TiO_2 surface shifts E_{CB} in a direction that decreases the energy difference between E_{CB} and E_{redox} because the monolayer consists of molecules with a dipole moment pointing away from

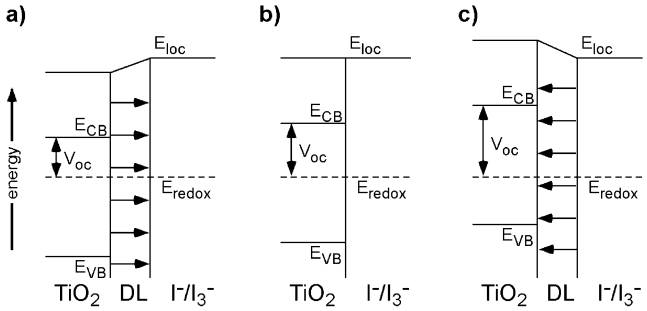

Figure 5. Energy band diagrams of TiO_2 nanoparticle/electrolyte interface with (a) a dipole layer (DL) composed of molecules with positive dipole moments at the interface (arrow points toward negative pole), (b) without dipole layer at the interface, and (c) with a dipole layer of negative dipole moment molecules at the interface: E_{loc}, local vacuum level; E_{CB}, bottom of the conduction band (CB); E_{VB}, top of the valence band (VB); E_{redox}, redox potential of the electrolyte; V_{oc}, open circuit voltage.

the TiO_2 surface (positive dipole). The situation with no dipole layers at the TiO_2/electrolyte interface is depicted in Figure 5b. An increased V_{oc} is observed if the molecules of the monolayer have a dipole moment which points toward the TiO_2 surface (negative dipole, Figure 5c). This explains qualitatively the correlation between the molecular dipole moment and the V_{oc}.

More quantitatively, we can calculate the electrostatic potential drop across the monolayer[27]according to

$$\Delta\phi_{\text{dipole}} = \frac{N\mu \cos\theta}{\epsilon\epsilon_o}$$

where N is the number of adsorbed molecules per surface area, μ is the molecular dipole moment, θ is the tilt angle between the axes of the dipole moment and the surface normal of the TiO_2 particles, ϵ is the dielectric constant of the monolayer, and ϵ_o is the dielectric permittivity of vacuum. For a coverage of 2×10^{13} cm^{-2} (corresponding to an area/adsorbed molecule of 500 Å^2, i.e., ∼8 times more than what was found for a monolayer of only benzoic or dicarboxylic acid derivatives on various semiconductors[28]), a 50−55° tilt angle ($\cos\theta \approx 0.6$) and a dielectric constant of $\epsilon = 5$,[16,28,12] we calculate a potential drop of $\Delta\phi/\mu = 9$ mV/D, which correlates well with the measured value of 6−9 mV/D. we note that for close to full coverage of benzoic acid on TiO_2 in the absence of any dye, $\Delta\phi/\mu$ was found to be about 200 mV/D.[18] This suggests an effective coverage is about 5% which agrees well with our estimate derived from optical absorption of the phosphonic acids.

Measurements of modified electrodes show that the V_{oc} of cells with dye-sensitized TiO_2 electrode without coadsorbed molecules does not fall on the linear fit to the other data. This is particularly pronounced for electrodes with coadsorbed phosphonic and dicarboxylic acid derivatives (Figure 4a,c). For the latter series the mismatch could be explained by the lower dye concentration of the modified electrodes. This results in a lower electron injection rate into the TiO_2, which subsequently leads to a lower V_{oc}, because, to a first approximation, the lower the injection rate, the farther the TiO_2 quasi-Fermi level will remain removed in energy from the bottom of the TiO_2 CB.[8,9] However, the other two series (Figure 4a,b), in which the dye surface concentrations are nearly constant, indicate that the mismatch between the V_{oc} of the unmodified reference samples and those with adsorbed acids cannot be due to the flux of photoinjected electrons into the TiO_2. Instead we suggest that it is caused by one of the following reasons:

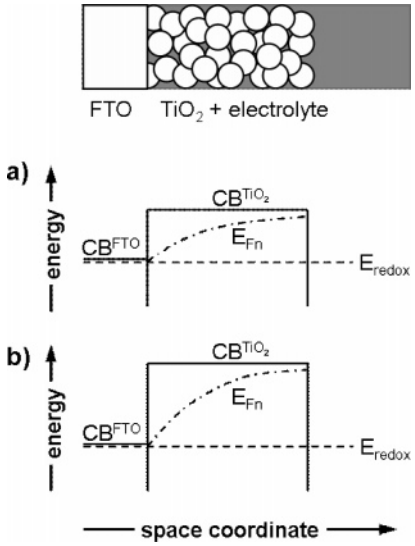

Figure 6. Schematic drawing of a DSSC cross-section that shows the mesoporous TiO_2 electrode immersed in the electrolyte and deposited on a conducting, F-doped SnO_2 substrate (FTO). (a) A shift of the TiO_2 conduction band (CB) toward E_{redox} results in a lower gradient of the electron quasi-Fermi level, E_{Fn}, and thus a smaller driving force for an electron current to the FTO substrate. (b) If the CB is shifted away from E_{redox}, the effect is reversed and the E_{Fn} gradient is increased. For simplicity the dipole at the TiO_2/electrolyte interface (the cause of the CB shift) is not shown explicitly. The way the Fermi levels change with space coordinate is drawn in (a) and (b) in a schematic fashion that does not take into account the microscopic effects. In reality, the variation of the quasi-Fermi level will be less monotonous because of that structure.

(1) The dipole moments were calculated for free molecules and did not include any charge rearrangement upon binding which subsequently can change the dipole moment. Within each series of molecules the binding group is the same such that the real dipole moments might be shifted by a constant amount relative to the calculated values. As a result the V_{oc} of the unmodified N3/TiO_2 film will match with the linear fit, if this uniform shift is toward more positive dipole moments (than those of the free molecules).

(2) The absorbed dye on the TiO_2 has a dipole moment,[29] which is more negative than the dipole moment of the coadsorbed molecules. If a very small amount of N3 molecules is replaced—small enough to leave the flux of photoinjected electrons unchanged but big enough to change the potential drop at the TiO_2/electrolyte interface—then the N3 reference measurement should not be plotted at 0 D but at a more negative value. Comparison of Figure 4a,b reveals that the reference measurement matches reasonably well the linear fit, when it is plotted at around −3 D.

To explain the dipole dependence of I_{sc} we propose two mechanisms, viz., a change in driving force for electron transport to the FTO substrate and a dipole-dependent recombination current. Both mechanisms are a consequence of a dipole-induced band shift.

Figure 6a,b show schematically the quasi Fermi level E_{Fn} at short circuit. A shift of E_{CB} toward E_{redox}, due to a more positive molecular dipole at the TiO_2/electrolyte interface, will decrease the driving force for electron transport toward the FTO substrate (shown as smaller E_{Fn} gradient in Figure 6a). In contrast, an upward shift of E_{CB}, caused by a negative molecular dipole moment, increases the gradient of E_{Fn}, as shown in Figure 6b, which results in a higher I_{sc}.

Additionally the shift of the energy levels can affect electron recombination from the TiO_2 into the electrolyte, which has an impact on I_{sc}. Electron recombination strongly depends on the energetic overlap of the TiO_2 states with the oxidized species of the electrolyte.[30] Figure 7 shows schematically the density of electronic states at E_{CB} as a function of energy (D_{CB}), an exponential trap density distribution below E_{CB}, and the density of states for the oxidized ($D_{ox.}$) and reduced species ($D_{red.}$) of the electrolyte. The energetic overlap of $D_{ox.}$ with TiO_2 CB states (solid gray) and band gap states (horizontally dashed) is depicted in Figure 7a,b for an interface without dipole layer and with dipole layer, respectively. The latter shifts the CB away from E_{redox} and decreases the overlap of the TiO_2 states with oxidized species of the electrolyte, which results in a lower recombination and a higher photocurrent. For a band shift toward E_{redox}, the overlap is increased and I_{sc} should be smaller due to increased recombination (not shown), which is in agreement with the experiments (Figure 4a−c).

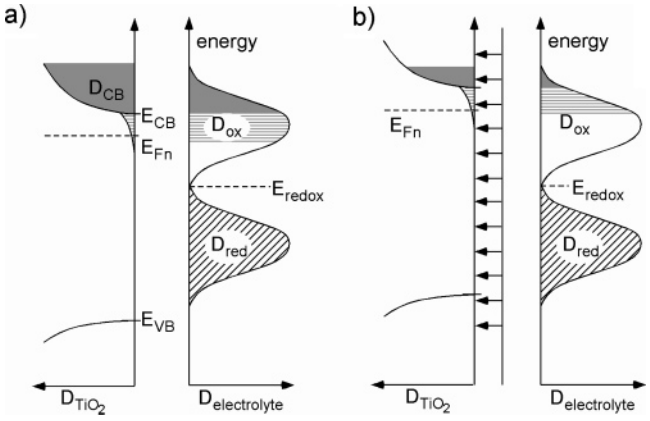

Figure 7. (a) Energy level alignment of the energy level distribution of oxidized ($D_{ox.}$) and reduced species ($D_{red.}$) of the electrolyte with the energy levels of the TiO_2 conduction band (D_{CB}). The filled gray parts show the CB energy levels, while the horizontal dashed parts show the gap states that overlap in energy space with the energy levels of the oxidized redox species, which contribute to electron transfer from the TiO_2 into the electrolyte. (b) Situation in the presence of a negative dipole layer on the TiO_2, which leads to decreased recombination due to a smaller overlap of the oxidized species with TiO_2 CB and gap states.

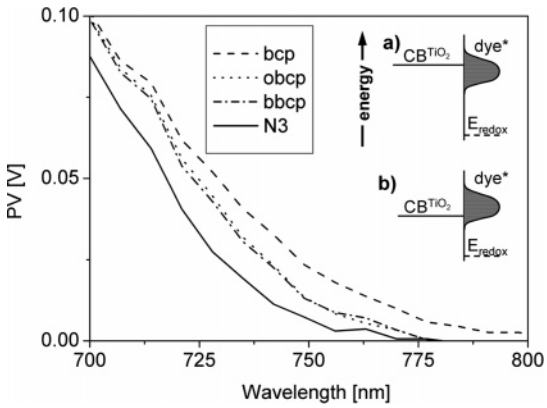

Figure 8. Photovoltage spectroscopy of dye-sensitized TiO_2 electrodes with molecular coadsorbed phosphonic acids. The insert shows how the energy levels of the excited dye state (dye*) can partly follow the dipole-related shift of the TiO_2 CB toward E_{redox}, which leads to a more pronounced overlap of the CB with dye* states in b compared to a.

Photovoltage Spectroscopy Measurements. Further support for the proposed dipole-related band shift comes from photovoltage spectroscopy (PVS) measurements. Figure 8 shows spectra for modified N3/TiO_2 electrodes with phosphonic acid derivatives. The onset of the photovoltage (PV) signal is shifted toward longer wavelengths if phosphonic acid derivatives are

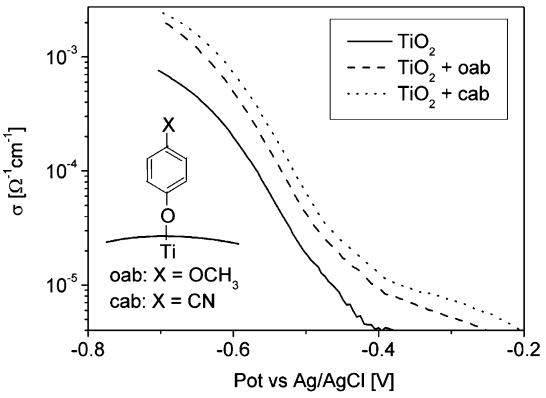

Figure 9. Conductivity plot of a bare, mesoporous TiO_2 film and molecular modified films with electrochemical deposited 4-methoxybenzenediazonium tetrafluoroborate (oab) and 4-cyanobenzenediazonium tetrafluoroborate (cab), schematically shown at the right side.

coadsorbed to the surface. This can be interpreted as a shift of E_{CB} toward E_{redox}, which is only partly followed by the dye molecules. The insert of Figure 8 shows the distributions of excited dye states (dye*) for an unmodified electrode (a) and a modified electrode with a lowered CB (b). The dye states are less shifted toward E_{redox} than the CB, which enables electron injection from excited dye states at lower energies. This CB shift is in qualitative agreement with the V_{oc} measurements (Figure 4a), which showed a systematic decrease in V_{oc}. From Figure 8 we derive that the shift of the PV onset is ~5.5 mV/D and thus about two-thirds of the V_{oc} shift, which indicates that the energy levels of the dye partly follow the shift of the TiO_2 bands. Similar effects have been reported in the literature for experiments where the ionic double layer (and thus the electrostatic potential) at the TiO_2/electrolyte interface was modified (by a change in the electrolyte composition and its pH).[31]

Conductivity Measurements of Molecular Modified TiO_2 Films. The photovoltage measurements of the surface dipole effect on the electrochemical semiconductor system discussed above were interpreted as dipole-induced CB potential shifts. To verify this approach further, we measured the effect of molecular modification of mesoporous TiO_2 electrodes on their electronic conductivity. The conductivity via the nanoporous TiO_2 network as a function of an external applied potential vs a Ag/AgCl reference electrode,[23] for a bare electrode and p-CH_3O (oab) and p-CN (cab) coated electrodes are shown in Figure 9.

Molecular modification improves the conductivity, irrespective of the direction of the molecular dipole (cab, positive; oab, negative). This can be explained by a shift of the TiO_2 bands with respect to the electrolyte potential, as is depicted in an energy diagram in Figure 10 for potentials U^{WE_1} and U^{WE_2}, applied to WE_1 and WE_2, respectively. The energy levels of the TiO_2 bands are adjusted with respect to the potential of the electrolyte (E_{ref}), which penetrates into the pores of the mesoporous structure of the film. This band alignment depends on the interface dipole at the TiO_2/electrolyte interface, as shown in Figure 10, and, thus, on the molecular dipole moment. The conductivity data shown in Figure 9 suggest that the TiO_2 CB is closer to the vacuum level without, than with, molecular surface modification of the TiO_2, if the data are interpreted by a pure band shift. The CB is shifted more strongly toward E_{ref} if the TiO_2 surface is modified with cab (Figure 10c) than if it is modified with oab molecules (Figure 10b). At the same applied potential (U^{WE_1}, U^{WE_2} vs E_{ref}) more mobile CB electrons are available for the cab-modified electrode than for the oab-

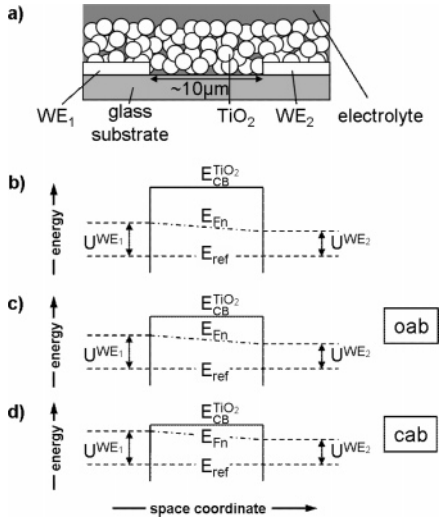

Figure 10. (a) Schematic drawing of a gap electrode, covered with a mesoporous TiO_2 film, immersed into electrolyte. (b) Energy band diagram to explain the dipole-related change of the conductivity for the unmodified TiO_2 film in contact with working electrode 1,WE_1, working electrode 2, WE_2 and the electrolyte at a negative applied potential vs Ag/AgCl ($=E_{ref}$). (c) The molecular modified electrode with oab molecules at the same applied potential. (d) Like c but with molecules with a more positive dipole moment (cab).

or unmodified one, shown by the energy difference between E_{Fn} and E_{CB} in Figure 10a−c. This results in higher conductivity of the cab- than the oab-modified electrode. We note that because the electrochemical method for anchoring molecules on the surface affects dye adsorption and leaves no room for significant dye coadsorption after anchoring of the molecules, it could not be used to study the effect of these types of molecules on the actual TiO_2 film with adsorbed dye.

Comparison between Dark Conductivity and Photocurrent and -voltage Results. The results from the conductivity measurements are in qualitative agreement with the observed dipole-dependent shift of the V_{oc}. It might seem contradictory that TiO_2 films modified with molecules with a dipole moment, which is lowering the CB, results in a higher conductivity but in a lower photocurrent density. The difference is that in one case the system is optically excited (I_{sc} measurements), while in the other case the system is measured in the dark (conductivity measurements). In the conductivity measurements the quasi-Fermi level is defined by the applied electrostatic potential to WE_1 and WE_2. For I_{sc} measurements, E_{Fn} in the TiO_2 depends on the electron injection rate, the recombination rate, and the current collection efficiency at the FTO substrate, which in turn depends on the gradient of E_{Fn}. The beneficial effect of an increased E_{Fn} gradient for I_{sc} has been discussed above. The results from I_{sc} and conductivity measurements indicate that the gradient effect of E_{Fn} has greater influence on DSSC operation than the dipole-induced change in the TiO_2 conductivity.

Conclusions

We have shown that molecular modification of mesoporous, dye-sensitized TiO_2 electrodes can be used for a systematic band alignment of the TiO_2 CB. The CB is shifted with respect to the electrolyte redox potential as a function of the dipole of the coadsorbed molecules. As a result, the V_{oc} is linearly dependent on the molecular dipole moment. The shift of the TiO_2 CB by the molecular dipole is also supported by conductivity measurements.

A dipole-related shift of the short-circuit current is explained by a dipole dependence of the driving force for electron current

as well as a dipole dependence of the recombination. The adsorbed dye follows only partly the shift of the TiO_2 bands, which can be seen from a shift in the signal onset of photovoltage spectroscopy measurements.

Molecular coadsorption can be used to align the TiO_2 CB level with respect to the excited states of the dye. This approach opens the possibility to improve electron injection efficiencies of alternative dye sensitizers for TiO_2-based DSSCs, which have a high density of excited states below the unmodified TiO_2 CB level. We note, though, that the use of such dyes will be at the expense of the V_{oc}.

Acknowledgment. S.R. acknowledges the financial support provided by the Minerva Foundation and the European Union's Human Potential Program under Contract No. HPRN-CT-2000-00141, ETA Solar Cells. D.C. acknowledges financial support from the Philip M. Klutznick Research Fund, the GMJ Schmidt Minerva Centre for Supramolecular Chemistry and the EU NoE PHOREMOST. A.Z. and M.G. acknowledge the financial support provided by the Israel Science Foundation founded by The Israel Academy of Science and Humanities. S.R. and M.G. contributed equally to this work.

References and Notes

(1) Grätzel, M. *J. Photochem. Photobiol., A* **2004**, *164*, 3.
(2) Rehm, J. M.; McLendon, G. L.; Nagasawa, Y.; Yoshihara, K.; Moser, J.; Grätzel, M. *J. Phys. Chem.* **1996**, *100*, 9577.
(3) Argazzi, R.; Bignozzi, C. A.; Heimer, T. A.; Castellano, F. N.; Meyer, G. J. *J. Phys. Chem. B* **1997**, *101*, 2591.
(4) Huang, S. Y.; Schlichthorl, G.; Nozik, A. J.; Grätzel, M.; Frank, A. J. *J. Phys. Chem. B* **1997**, *101*, 2576−2582.
(5) Heimer, T. A.; Darcangelis, S. T.; Farzad, F.; Stipkala, J. M.; Meyer, G. J. *Inorg. Chem.* **1996**, *35*, 5319.
(6) Nazeeruddin, M. K.; Humphrybaker, R.; Liska, P.; Grätzel, M. *J. Phys. Chem. B* **2003**, *107*, 8981.
(7) Zaban, A.; Ferrere, S.; Sprague, J.; Gregg, B. A. *J. Phys. Chem. B* **1997**, *101*, 55.
(8) Bisquert, J.; Cahen, D.; Hodes, G.; Rühle, S.; Zaban, A. *J. Phys. Chem. B* **2004**, *108*, 8106.
(9) Cahen, D.; Hodes, G.; Grätzel, M.; Guillemoles, J. F.; Riess, I. *J. Phys. Chem. B* **2000**, *104*, 2053.
(10) Lenzmann, F.; Krüger, J.; Burnside, S.; Brooks, K.; Grätzel, M.; Gal, D.; Rühle, S.; Cahen, D. *J. Phys. Chem. B* **2001**, *105*, 6347.
(11) Cohen, R.; Kronik, L.; Shanzer, A.; Cahen, D.; Liu, A.; Rosenwaks, Y.; Lorenz, J. K.; Ellis, A. B. *J. Am. Chem. Soc.* **1999**, *121*, 10545.
(12) Salomon, A.; Berkovich, D.; Cahen, D. *Appl. Phys. Lett.* **2003**, *82*, 1051.
(13) Gal, D.; Sone, E.; Cohen, R.; Hodes, G.; Libman, J.; Shanzer, A.; Schock, H. W.; Cahen, D. *Proc.−Indian Acad. Sci., Chem. Sci.* **1997**, *109*, 487.
(14) Visoly-Fisher, I.; Sitt, A.; Wahab, M.; Cahen, D. *ChemPhysChem* **2005**, *6*, 277.
(15) Vilan, A.; Shanzer, A.; Cahen, D. *Nature* **2000**, *404*, 166.
(16) Vilan, A.; Ghabboun, J.; Cahen, D. *J. Phys. Chem. B* **2003**, *107*, 6360.
(17) Selzer, Y.; Cahen, D. *Adv. Mater.* **2001**, *13*, 508.
(18) Krüger, J.; Bach, U.; Grätzel, M. *Adv. Mater.* **2000**, *12*, 447.
(19) Zaban, A.; Aruna, S. T.; Tirosh, S.; Gregg, B. A.; Mastai, Y. *J. Phys. Chem. B* **2000**, *104*, 4130.
(20) Merson, A.; Dittrich, T.; Zidon, Y.; Rappich, J.; Shapira, Y. *Appl. Phys. Lett.* **2004**, *85*, 1075.
(21) Meulenkamp, E. A. *J. Phys. Chem. B* **1999**, *103*, 7831.
(22) Roest, A. L.; Kelly, J. J.; Vanmaekelbergh, D.; Meulenkamp, E. A. *Phys. Rev. Lett.* **2002**, *89*.
(23) Abayev, I.; Zaban, A.; Fabregat-Santiago, F.; Bisquert, J. *Phys. Status Solidi A* **2003**, *196*, R4.
(24) Nazeeruddin, M. K.; Kay, A.; Rodicio, I.; Humphrybaker, R.; Muller, E.; Liska, P.; Vlachopoulos, N.; Gratzel, M. *J. Am. Chem. Soc.* **1993**, *115*, 6382.
(25) Pichot, F.; Gregg, B. A. *J. Phys. Chem. B* **2000**, *104*, 6.
(26) Rühle, S.; Cahen, D. *J. Phys. Chem. B* **2004**, *108*, 17946.
(27) Kronik, L.; Shapira, Y. *Surf. Sci. Rep.* **1999**, *37*, 1.
(28) Ashkenasy, G.; Cahen, D.; Cohen, R.; Shanzer, A.; Vilan, A. *Acc. Chem. Res.* **2002**, *35*, 121.
(29) Zuppiroli, L.; Si-Ahmed, L.; Kamaras, K.; Nuesch, F.; Bussac, M. N.; Ades, D.; Siove, A.; Moons, E.; Gratzel, M. *Eur. Phys. J. B* **1999**, *11*, 505.
(30) Bisquert, J.; Zaban, A.; Greenstein, M.; Mora-Seró, I. *J. Am. Chem. Soc.* **2004**, *126*, 13550.
(31) Zaban, A.; Ferrere, S.; Gregg, B. A. *J. Phys. Chem. B* **1998**, *102*, 452.